JGR Space Physics

RESEARCH ARTICLE
10.1029/2020JA028387

A Statistical Survey of Low-Frequency Magnetic Fluctuations at Saturn

Dong-Xiao Pan[1], Zhong-Hua Yao[1], Rui-Long Guo[2], Bertrand Bonfond[2], Yong Wei[1], William Dunn[3], Bin-Zheng Zhang[4], Qiu-Gang Zong[5], Xu-Zhi Zhou[5], Denis Grodent[2], and Wei-Xing Wan[1]

[1]Key Laboratory of Earth and Planetary Physics, Institute of Geology and Geophysics, Chinese Academy of Sciences, Beijing, China, [2]Laboratoire de Physique Atmospherique et Planetaire, STAR Institute, Universite de Liege, Liege, Belgium, [3]University College London, Mullard Space Science Laboratory, Dorking, UK, [4]Department of Earth Sciences, the University of Hong Kong, Hong Kong SAR, China, [5]School of Earth and Space Sciences, Peking University, Beijing, China

Key Points:

- Using the complete Cassini magnetometer data set, we present the global picture of ultralow frequency waves in Saturn's magnetosphere
- The wave power shows a rapid decrease beyond 25 R_S in both the morning and afternoon sectors
- The wave activity peaks in noon sector, implying that these waves could be driven by the solar wind interaction with Saturn's magnetopause

Supporting Information:

- Supporting Information S1
- Figure S1
- Figure S2

Correspondence to:
Z.-H. Yao,
z.yao@ucl.ac.uk

Citation:
Pan, D.-X., Yao, Z.-H., Guo, R.-L., Bonfond, B., Wei, Y., Dunn, W., et al. (2021). A statistical survey of low-frequency magnetic fluctuations at Saturn. *Journal of Geophysical Research: Space Physics*, *126*, e2020JA028387. https://doi.org/10.1029/2020JA028387

Received 22 JUN 2020
Accepted 15 DEC 2020

Abstract Low-frequency waves are closely related to magnetospheric energy dissipation processes. The Cassini spacecraft explored Saturn's magnetosphere for over 13 years, until September 2017, covering a period of more than a complete solar cycle. Using this rich heritage data set, we systematically investigated key physical parameters of low-frequency waves in Saturn's magnetosphere, including their local time distribution and the dependence on solar activity. We found that the wave activity peaked in the near noon sector. For the nightside, the wave intensity also appeared to peak pre and postmidnight. Due to the limited local time coverage for each solar phase, we were not able to draw a firm conclusion on the wave's dependence on solar activity. In general, the wave power showed a monotonically decreasing trend toward larger distances in nightside sectors especially during the declining phase, which implied that low-frequency waves mainly originate from the relatively inner regions of the magnetosphere. On the dayside, stronger waves were mostly located at/within ~25 R_S, near the magnetopause. The study shows a global picture of low-frequency waves in Saturn's magnetosphere, providing important implications for how magnetospheric energy dissipates into Saturn's polar ionosphere and atmosphere.

1. Introduction

For the terrestrial magnetosphere the plasma source is predominately the solar wind via the Dungey cycle process (Dungey, 1961). In contrast, the particle source for Saturn's outer magnetosphere is escaping water vapor from its moon Enceladus (Blanc et al., 2015; Hansen et al., 2006; Waite et al., 2006), which drives Saturn's magnetospheric processes. Despite different energy sources at each planet, similarities are found in many fundamental processes. For example, magnetic reconnection and dipolarization processes are fundamental plasma processes in accelerating and circulating particles in the magnetosphere, and they are found at Earth (Akasofu, 2017; Angelopoulos et al., 2008; Baker et al., 1996), Mercury (Slavin et al., 2009; Sun et al., 2015), Saturn (Jackman et al., 2007, 2015; Z. H. Yao, Grodent, et al., 2017) and Jupiter (Russell et al., 1998; Vogt et al., 2010; Z. H. Yao et al., 2019). Recent studies also reveal similar auroral structures between Saturn and Earth (Radioti et al., 2017, 2019; Z. Yao, Pu, et al., 2017), due to the similar processes.

Among the similarities between planetary magnetospheric processes, low-frequency plasma waves, also known as ultralow frequency waves (Chen, 1999; Hasegawa & Chen, 1974; Lee & Lysak, 1989; Q. G. Zong et al., 2009), have been extensively investigated at different planets (Glassmeier et al., 2004; Kleindienst et al., 2009), as they are fundamental perturbations in magnetized plasma environments. Due to the very different sizes of planetary magnetospheres, the eigenfrequency of magnetic field line resonances between the northern and southern hemispheres can vary significantly from planet to planet. For example, the fundamental periods of magnetic field line resonances at Earth are usually a few minutes, while the fundamental periods for Mercury are a few seconds and for the giant planets they can be tens of minutes (Glassmeier et al., 2004; Kleindienst et al., 2009). Despite the large difference in temporal scales, the fundamental physical processes are similar.

The low-frequency waves at Saturn are generated by various processes. Kelvin-Helmholtz vortices, a consequence of solar wind-magnetosphere interaction, are often formed on Saturn's dawnside magnetopause,

which could systematically excite field line resonances (Delamere et al., 2013; Masters et al., 2009, 2010). The plasma circulation from Vasyliunas (internally driven) reconnection may also be an energy source to excite magnetic field line resonances (Z. H. Yao, Radioti, et al., 2017). Furthermore, solar wind compressions could also directly form compressional mode waves on the magnetopause, and the wave would transform into shear Alfvén waves when propagating toward the inner magnetosphere (Allan & Poulter, 1992; Q. Zong et al., 2017). To date, it is unclear whether or not there is a systematic correlation between solar activity and Saturn's low-frequency wave activities. In this study, the low-frequency waves at Saturn are defined as magnetic perturbations at periods of 10–60 min.

The low-frequency fluctuations have been identified not only from magnetic field measurements, but also from aurora and energetic particle observations, indicating that these fluctuations are global processes from the magnetosphere to the ionosphere and atmosphere. Quasiperiodic 1-h pulsations are found at Saturn's cusp aurora (Palmaerts, Radioti, et al., 2016). Such pulsations are believed to be connected to in situ observations of particle pulsations in the magnetosphere, which have similar periodicities (Palmaerts, Roussos, et al., 2016; Roussos et al., 2016). The Kelvin-Helmholtz instability is often considered to be a plausible mechanism for these pulsations. A recent study suggests that rotationally driven magnetodisc reconnection could also trigger such pulsations (Guo, Yao, Wei, et al., 2018), although the detailed connections are yet to be understood.

Throughout its mission, the Cassini spacecraft collected in situ magnetic field data from Saturn throughout an entire solar cycle. The large data set allows us to perform a systematic investigation of Saturn's low-frequency magnetic fluctuations, including local time distributions and the dependence on solar activity. In this study, we perform a statistical survey of low-frequency magnetic perturbations (with periods between 10 and 60 min) using the large Cassini magnetometer (MAG) data set (Dougherty et al., 2004).

2. Cassini Observations From 2005 to 2014: Dependence on Solar Activity

We investigate low-frequency magnetic fluctuations at Saturn from 2005 to 2014. Based on the 27-day averaged sunspot number adopted from the omni data set (Figure 1a), we further select four subsets from the Cassini MAG observations to represent different solar cycle phases. Each subset includes measurements during a two-year exploration, that is, during the declining phase (2005–2006), solar minimum (2008–2009), ascending phase (2010–2011), and solar maximum (2013–2014), respectively. Figures 1b–1i present Cassini trajectories for the four subsets in Kronocentric Solar Magnetospheric (KSM) system. During the selected 8 years, Cassini's trajectory covered an extensive area, including all local times and with radial distance up to $\sim 65 R_S$ ($1 R_S = 60{,}268$ km). Nevertheless, we need to bear in mind that the Cassini orbits show a significant bias toward specific local times and radial distances at each solar phase, which could superpose the effects of solar activity and spatial variations.

To conduct the statistical analysis on low-frequency magnetic fluctuations, we applied the Lomb-Scargle periodogram method (Lomb, 1976; Scargle, 1982) to obtain the power spectral density (PSD) of the fluctuating magnetic field with a 6-h window. Figure 2 shows an example of a wave event that occurred on October 28, 2015. Figures 2a and 2b present the trajectories of Cassini during this period. We used 6-h averaged magnetic field measurements to represent the background magnetic field (red line in Figure 2c). Figure 2e shows the power spectrum density of the detrended magnetic field (Figure 2d). The red horizontal line is the power-level threshold that is consistent with a probability of detection of 0.99, significantly lower than the observed wave power at specific frequencies. A wave event is thus selected when the probability of detection exceeds 0.99 to ensure that the peak in the spectrum is not due to random fluctuations. For each event, we define the mean value of PSD within the periods between 10 and 60 min, as the wave intensity $\mathrm{PSD_{wave}}$.

We systematically investigate Saturn's low-frequency magnetic fluctuations and their dependence on solar activity. Figure 3 shows the $\mathrm{PSD_{wave}}$ distributions of low-frequency waves during different solar phases and strong wave (with $\mathrm{PSD_{wave}}$ above 10^3 $\mathrm{nT^2/Hz}$) occurrence rates. The abscissa are the equatorial distances D ($D = \pm\sqrt{X_{KSM}^2 + Y_{KSM}^2}$) from Saturn in $X_{\mathrm{KSM}} - Y_{\mathrm{KSM}}$ plane. The dayside wave events are selected to be those where the local time ranges from 9 to 15. The blue dots are events at low latitude with $|Z_{\mathrm{KSM}}| < 5\ R_S$, and

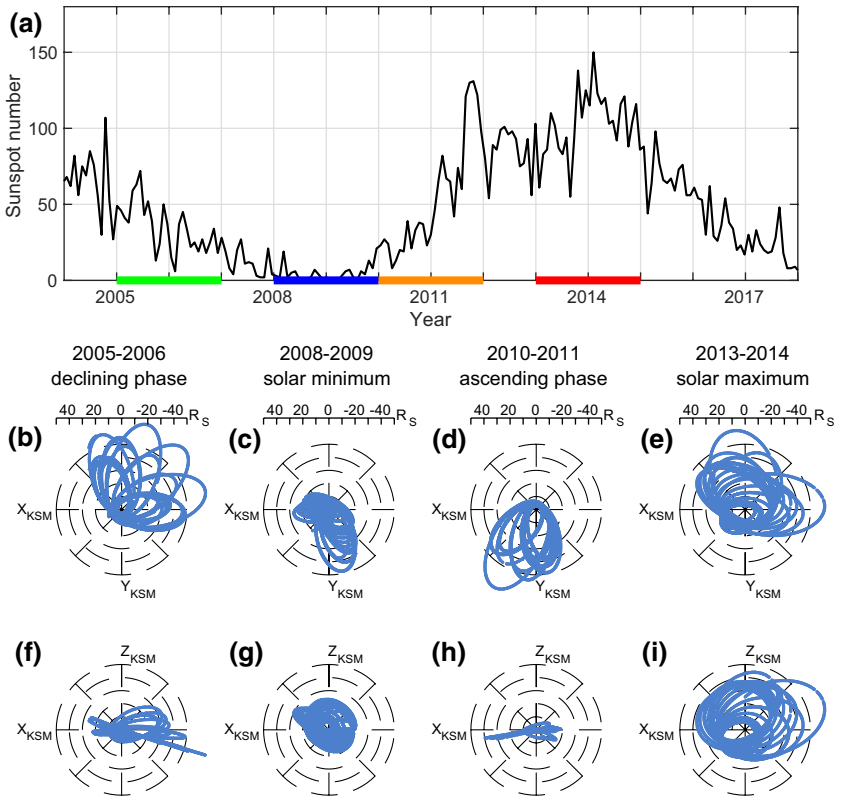

Figure 1. (a) Twenty seven-day averaged sunspot number from 2004 to 2017 adopted from omni data set (http://omniweb.gsfc.nasa.gov/), the color bars mark the four solor phases; (b–i) Cassini trajectories during declining phase, solar minimum, ascending phase and solar maximum (in KSM coordinates, where X directs to the Sun, $X-Z$ plane contains Saturn's centered magnetic dipole axis and Y completes right handed set). KSM, Kronocentric Solar Magnetospheric.

red dots are events at high latitude with $|Z_{KSM}| > 5\ R_S$. The black stars are the median value of PSD_{wave} for each bin, while the upper (lower) boundaries of shaded areas are consistent with the upper (lower) quartiles, displaying the overall trend of the data. We note that events with large PSD_{wave} ($>10^3$ nT^2/Hz) at the dayside sector are mostly located at/within $\sim 25R_S$, indicating strong wave activities near/within magnetopause. The PSD_{wave} and the occurrence rates of these strong waves at dayside (~40%) are similar for the four solar cycle phases. The PSD_{wave} also shows a decreasing trend for $D > 30\ R_S$ as shown in Figures 3e and 3g. The nightside wave power spectrum density is monotonically decreasing toward large distances during the declining phase (Figure 3a) and is largely scattered with a relatively low mean value during the solar maximum phase (Figure 3g). There was insufficient data to obtain the trend in the nightside for the other two solar phases (Figures 3c and 3e), so that it is hard to study the day-night asymmetry or compare the nightside wave activities.

Figure 4 focuses on events located in the dawn sector (03–09 LT) and the dusk sector (15–21 UT). The positive value of the abscissas in Figure 4 represent the dusk sector ($Y_{KSM} > 0$). The wave intensity decreases with increasing equatorial distances D, in both the dawnside (Figures 4a and 4g) and the duskside (Figures 4c and 4e) for each phase of the solar cycle. The PSD_{wave} distributions for events at high latitude (red dots) are usually much more dispersed than those events at low latitude (blue dots). We noted that the bias of the Cassini orbits strongly mixes the effects of solar activities and spatial variations so that it is hard to compare the dawnside/duskside wave activities. In addition, we used electron data with energy up to 28 keV provided by Cassini-CAPS (Young et al., 2004), to examine the wave intensity distribution inside the magnetopause. We analyzed the events with an electron temperature greater than 100 eV, as the electron temperature in the magnetosheath is well below this value (Figures S1 and S2). The results show that only

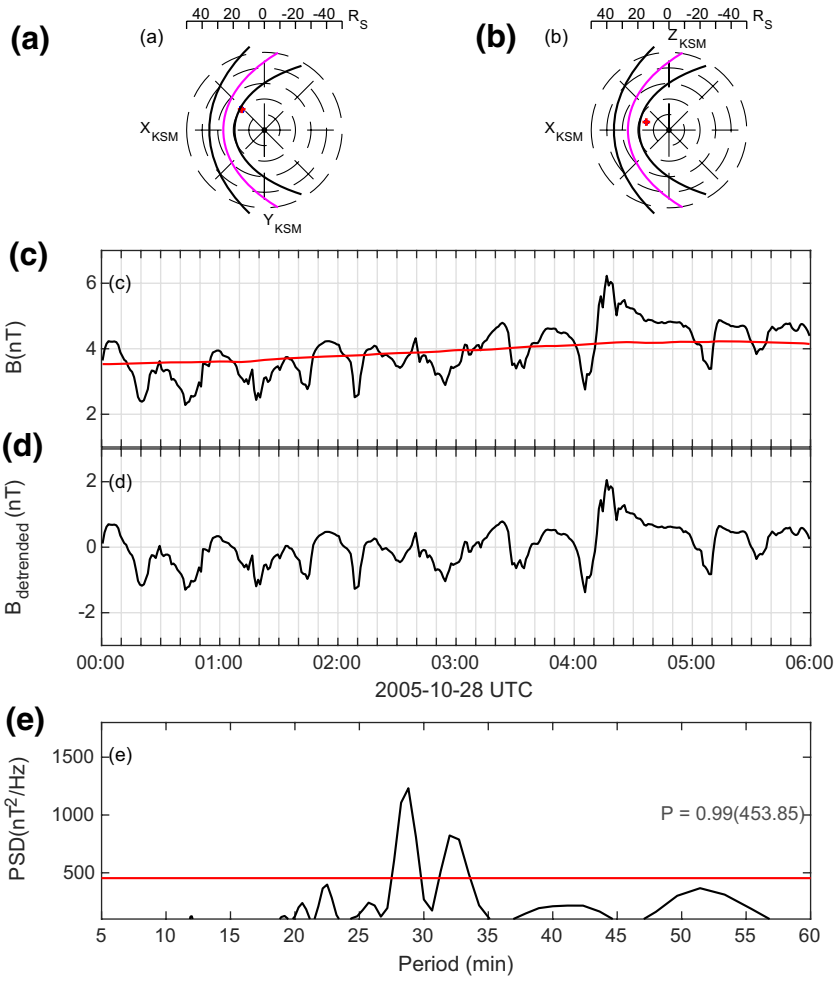

Figure 2. An example wave event on October 28, 2005. Cassini locations represented by red dots on (a) $X_{KSM} - Y_{KSM}$ and (b) $X_{KSM} - Z_{KSM}$ plane; The magenta and black curves are potential and possible magnetopause positions based on the A06 model with improved parameters for solar wind pressure of 0.00906 nPa (Guo, Yao, Wei, et al., 2018; Kanani et al., 2010) (c) The intensity of the magnetic field detected by Cassini MAG instrument. The red curve represents background magnetic field, obtained from 6-h running average. (d) The detrended magnetic field and (e) power spectral density (PSD) for the detrended magnetic field which is obtained from the Lomb-Scargle periodogram method. The red horizontal line shows power-level thresholds that are consistent with a probability of detection equal to 0.99.

intense waves remained, implying that most of the weak waves ($PSD_{wave} < 10^3$ nT^2/Hz) are from the magnetosheath, which is consistent with the results in Figure 5 (shown later).

3. An Overview: Dependence on Local Time

In this section, we combine data from all subsolar phases as marked in Figure 1 to investigate the dependence of wave activity with spatial variations. Figure 5a and 5b shows the distribution of the wave events on the $X_{KSM} - Y_{KSM}$ and $X_{KSM} - Z_{KSM}$ plane combining the data from all four subsets. Each dot represents a wave event and the color represents the wave intensity. The magenta curve predicted the magnetopause position calculated from the A06 model with improved parameters (Kanani et al., 2010) using the solar wind pressure of 0.00906 nPa (Guo, Yao, Sergis, et al., 2018; Guo, Yao, Wei, et al., 2018). The inner and outer black curves represent the possible magnetopause positions corresponding to the root mean square errors of the A60 model coefficients. It is clear that the wave activity is strong near $\sim 25R_S$ and inside, especially near the subsolar point. We find that the wave activity rapidly decreases outside of $\sim 25R_S$ at dayside, which

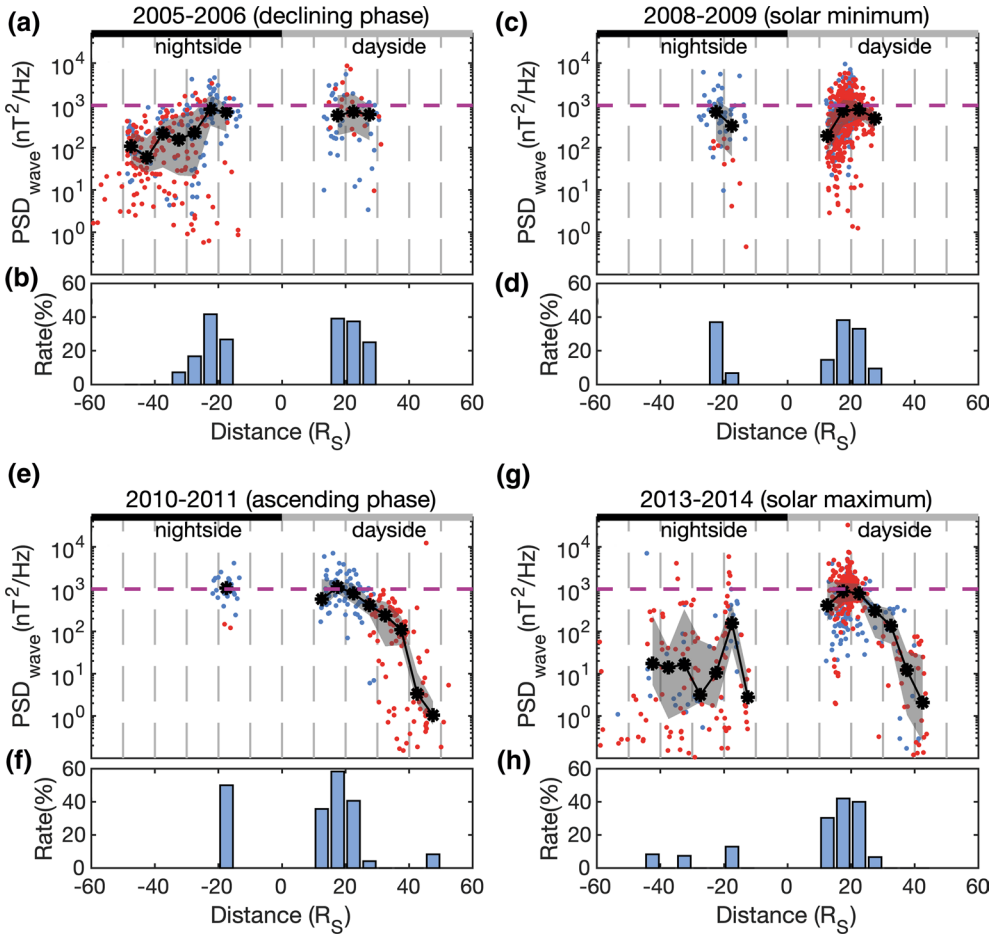

Figure 3. Scatterplots of low-frequency waves PSD_{wave} versus equatorial distances D from Saturn (positive when $X_{KSM} > 0$; negative when $X_{KSM} < 0$) and the occurrence rates for intense waves in different regions, during (a–b) declining phase, (c–d) solar minimum, (e–f) ascending phase and (g–h) solar maximum. The dayside sectors contain events in the local time range of 9–15 LT, while nightside events are in the local time range of 21–03 LT. Blue dots are events with $|Z_{KSM}| < 5R_S$, while red dots are events with $|Z_{KSM}| > 5R_S$. The black stars represent the median value of PSD_{wave} for each bin and the shaded areas mark events between upper quartile and lower quartile. Each bin contains at least 10 data points. Blue bar charts show occurence rates for intense waves, which are defined as the number of events with $PSD_{wave} > 10^3$ nT^2/Hz divided by the number of all events in each bin.

is consistent with the nominal magnetopause location (Kanani et al., 2010). We would like to point out that there is little data along the subsolar line at >25 R_S, but the trend is clear in both the morning and afternoon sectors, implying that low-frequency waves are magnetospheric as opposed to a magnetosheath or solar wind process. The main periods of these intense waves are 30–60 min, shown in Figure 5c.

Figure 5d shows the PSD_{wave} as a function of local time with events located at a distance D ranging from $20R_S$ to $30R_S$. The gray dots represent the wave events. The red stars are the median value of PSD_{wave} for each local time, while blue bars represent the occurrence rate of intense waves. The wave activity peaks in the noon sector, implying that solar wind's interaction with Saturn's magnetopause is an important mechanism in driving the magnetospheric low-frequency waves. Magnetopause surface waves (Masters et al., 2009, 2012; Cutler et al., 2011; Lepping et al., 1981) and/or Kelvin-Helmholtz waves (Wilson et al., 2012) caused by the interactions between the solar wind and Saturn's magnetopause are likely the major contributions. We also noted that the wave intensity also peaks at premidnight and postmidnight. The driver for nightside waves is inconsistent with the magnetopause surface waves. Nightside waves may instead be a consequence of Titan torus perturbation or nightside transient plasma processes (e.g., magnetic reconnection or bursty bulk flows).

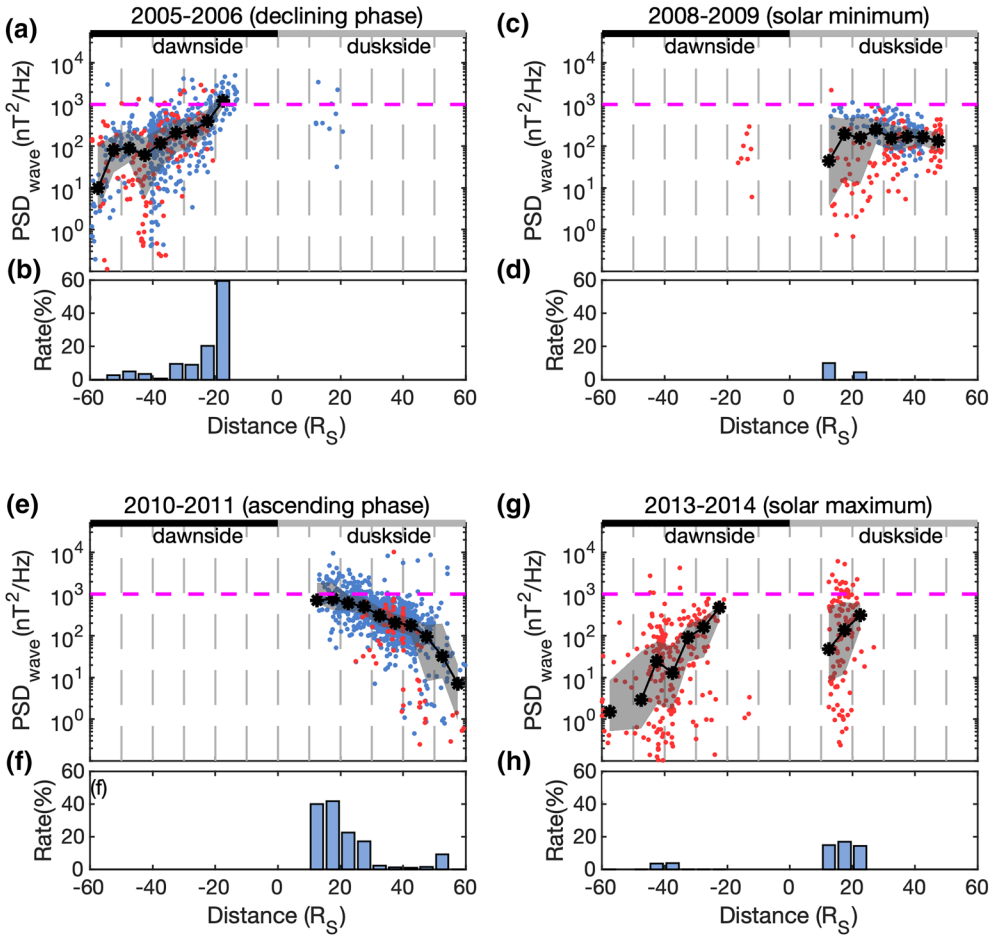

Figure 4. Same format as Figure 3, but for dawnside and duskside events. The abscissas represent equatorial distances D from Saturn (positive when $Y_{KSM} > 0$; negative when $Y_{KSM} < 0$). The dawnside sectors contain events within the range 03–09 LT, while the duskside sectors are defined as events in the local time range 15–21 LT.

4. Conclusions

Low-frequency wave activity is a consequence of many fundamental magnetospheric processes that perturb the magnetic field, energetic particles, auroral emissions, and so on. In this study, the low-frequency waves are selected only based on the periodicity. There are many proposed mechanisms for driving these waves, for example, K-H instabilities or solar wind pressure pulses. Since the wave power peaks near the magnetopause, we suggest the interaction between the solar wind and the rotating magnetosphere to be pivotal for the wave generation. These waves are associated with macro-processes, thus they are likely MHD waves. However, the interaction between the solar wind and the rotating magnetosphere can also modify particle distribution and this may induce kinetic effects. The limited data coverage in local times for each solar phase does not allow us to draw a firm conclusion on a connection with solar activity. Nevertheless, no significant dependence on solar activity is identified from the existing data set. The results also show that dayside wave activity is generally stronger than at nightside near solar maximum, probably indicating the presence of a systematic wave driver on the magnetopause. It is clear that the wave power rapidly decreases beyond $\sim 25 R_S$ at morning and afternoon sectors, indicating that the detected waves are not from the magnetosheath or solar wind.

In analyzing the local time sectors, we found that a peak wave power was found near the noon sector, which is probably related to the active auroral region in the prenoon sector (Bader et al., 2019). The dayside wave distribution might also be related to drizzle-like reconnection, which also displays a peak occurrence

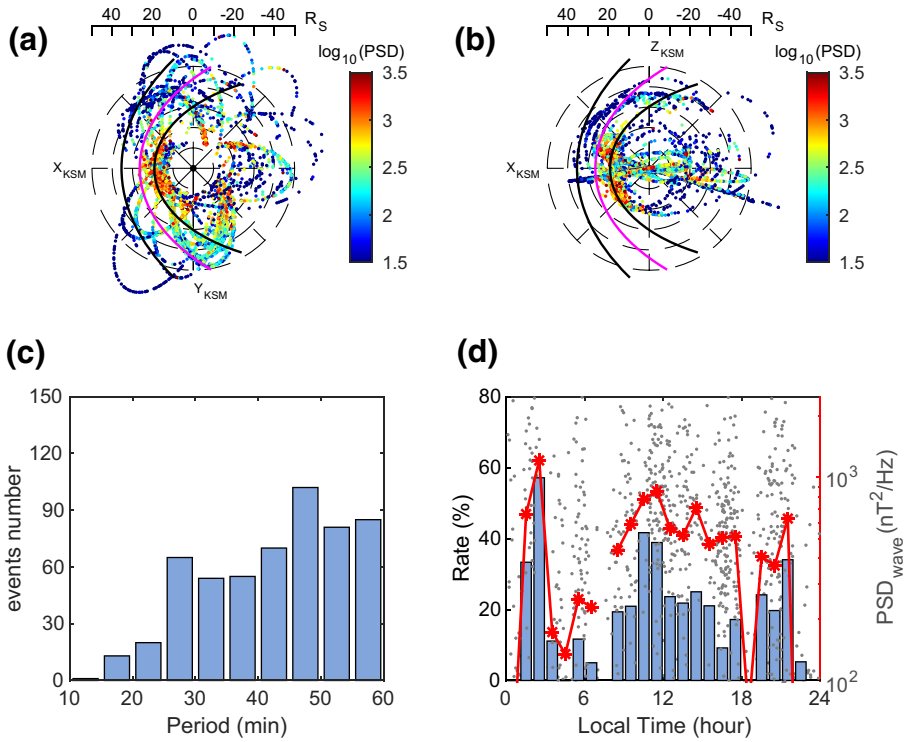

Figure 5. Low-frequency wave activity distributions on (a) $X_{KSM} - Y_{KSM}$ and (b) $X_{KSM} - Z_{KSM}$ plane. The color scheme represents the magnitude of $\log_{10}PSD_{wave}$.The magenta and black curves are potential and possible magnetopause positions based on A06 model with improved parameters for solar wind pressure of 0.00906 nPa (Guo, Yao, Wei, et al., 2018; Kanani et al., 2010) (c) The distribution of periods for intense waves ($PSD_{wave} > 10^3$ nT^2/Hz) (d) The dependence of low-frequency wave power spectrum density with local time. Each gray dot represents a wave event, and red stars gives the median value of PSD_{wave} for each local time for the events located at distance D from $20R_S$ to $30R_S$. Blue bars represent the occurrence rate of intense waves for each local time.

probability near noon (Delamere et al., 2015). Auroral observations suggest pulsating auroral emissions with a periodicity of ~60 min (Palmaerts, Radioti, et al., 2016), which is consistent with the wave periodicities shown in this study. Our results suggest that low-frequency waves could be an important source of auroral emission at Saturn, as was proposed at Earth (Keiling et al., 2003, 2019; Zhao et al., 2019) and Jupiter (Saur et al., 2018). A further study combining magnetic perturbations and auroral images will help to answer this question. It is also worth conducting a magnetohydrodynamic (MHD) simulation to examine the importance of Alfvénic precipitation in driving auroral emissions.

Data Availability Statement

The Cassini data presented in this study are available at http://pds-ppi.igpp.ucla.edu/.

Acknowledgments
This work was supported by the Strategic Priority Research Program of Chinese Academy of Sciences (Grant No. XDA17010201) and National Natural Science Foundation of China (42004149, 41704169, 42074211). R.L.G. is supported by the Incoming Post-Docs in Sciences, Technology, Engineering, Materials and Agrobiotechnology (IPD-STEMA) project from Université de Liège. Denis Grodent and Bertrand

References

Akasofu, S.-I. (2017). Auroral substorms: Search for processes causing the expansion phase in terms of the electric current approach. *Space Science Reviews*, *212*(1–2), 341–381. https://doi.org/10.1007/s11214-017-0363-7

Allan, W., & Poulter, E. M. (1992). ULF waves-their relationship to the structure of the Earth's magnetosphere. *Reports on Progress in Physics*, *55*(5), 533–598. https://doi.org/10.1088/0034-4885/55/5/001

Angelopoulos, V., McFadden, J. P., Larson, D., Carlson, C. W., Mende, S. B., Frey, H., et al. (2008). Tail reconnection triggering substorm onset. *Science*, *321*(5891), 931–935. https://doi.org/10.1126/science.1160495

Bader, A., Badman, S. V., Cowley, S. W. H., Yao, Z. H., Ray, L. C., Kinrade, J., et al. (2019). The dynamics of saturn's main aurorae. *Geophysical Research Letters*, *46*(17–18), 10283–10294. https://doi.org/10.1029/2019GL084620

Baker, D., Pulkkinen, T., Angelopoulos, V., Baumjohann, W., & McPherron, R. (1996). Neutral line model of substorms: Past results and present view. *Journal of Geophysical Research*, *101*(A6), 12975–13010. https://doi.org/10.1029/95JA03753

Bonfond are supported by the PRODEX program managed by ESA in collaboration with the Belgian Federal Science Policy Office. William Dunn was supported by a Science and Technology Facilities Council (STFC) research grant to University College London (UCL) and by European Space Agency (ESA) contract no. 4000120752/17/NL/MH. The authors wish to thank the International Space Science Institute in Beijing (ISSI-BJ) for supporting and hosting the meetings of the International Team on "The morphology of auroras at Earth and giant planets: characteristics and their magnetospheric implications," during which the discussions leading/contributing to this publication were held. It was also made possible by the Key Research Program of the Institute of Geology and Geophysics CAS (grant IGGCAS-201904).

Blanc, M., Andrews, D. J., Coates, A. J., Hamilton, D. C., Jackman, C. M., Jia, X., et al. (2015). Saturn plasma sources and associated transport processes. *Space Science Reviews*, *192*(1–4), 237–283. https://doi.org/10.1007/s11214-015-0172-9

Chen, L. (1999). Theory of plasma transport induced by low-frequency hydromagnetic waves. *Journal of Geophysical Research*, *104*(A2), 2421–2427. https://doi.org/10.1029/1998JA900051

Cutler, J. C., Dougherty, M. K., Lucek, E., & Masters, A. (2011). Evidence of surface wave on the dusk flank of Saturn's magnetopause possibly caused by the Kelvin-Helmholtz instability. *Journal of Geophysical Research*, *116*, A10220. https://doi.org/10.1029/2011JA016643

Delamere, P. A., Otto, A., Ma, X., Bagenal, F., & Wilson, R. J. (2015). Magnetic flux circulation in the rotationally driven giant magnetospheres. *Journal of Geophysical Research*, *120*(6), 4229–4245. https://doi.org/10.1002/2015JA021036

Delamere, P. A., Wilson, R. J., Eriksson, S., & Bagenal, F. (2013). Magnetic signatures of Kelvin-Helmholtz vortices on Saturn's magnetopause: Global survey. *Journal of Geophysical Research*, *118*(1), 393–404. https://doi.org/10.1029/2012JA018197

Dougherty, M., Kellock, S., Southwood, D., Balogh, A., Smith, E., Tsurutani, B., et al. (2004). The cassini magnetic field investigation. *Space Science Reviews*, *114*(1–4), 331–383. https://doi.org/10.1007/s11214-004-1432-2

Dungey, J. (1961). Interplanetary magnetic field and auroral zones. *Physical Review Letters*, *6*(2), 47. https://doi.org/10.1103/PhysRevLett.6.47

Glassmeier, K.-H., Klimushkin, D., Othmer, C., & Mager, P. (2004). Ulf waves at mercury: Earth, the giants, and their little brother compared. *Advances in Space Research*, *33*(11), 1875–1883. https://doi.org/10.1016/j.asr.2003.04.047

Guo, R. L., Yao, Z. H., Sergis, N., Wei, Y., Roussos, E., et al. (2018). Reconnection acceleration in Saturn's dayside magnetodisk: A multicase study with cassini. *The Astrophysical Journal Letters*, *868*(2), L23. https://doi.org/10.3847/2041-8213/aaedab

Guo, R.-L., Yao, Z.-H., Wei, Y., Ray, L. C., Rae, I. J., Arridge, C. S., et al. (2018). Rotationally driven magnetic reconnection in saturn's dayside. *Nature Astronomy*, *2*(8), 640–645. https://doi.org/10.1038/s41550-018-0461-9AUG.

Hansen, C., Esposito, L., Stewart, A., Colwell, J., Hendrix, A., Pryor, W., et al. (2006). Enceladus' water vapor plume. *Science*, *311*(5766), 1422–1425. https://doi.org/10.1126/science.1121254

Hasegawa, A., & Chen, L. (1974). Theory of magnetic pulsations. *Space Science Reviews*, *16*(3), 347–359. https://doi.org/10.1007/BF00171563

Jackman, C. M., Russell, C. T., Southwood, D. J., Arridge, C. S., Achilleos, N., & Dougherty, M. K. (2007). Strong rapid dipolarizations in Saturn's magnetotail: In situ evidence of reconnection. *Geophysical Research Letters*, *34*(11), LL1023. https://doi.org/10.1029/2007GL029764

Jackman, C. M., Thomsen, M. F., Mitchell, D. G., Sergis, N., Arridge, C. S., Felici, M., et al. (2015). Field dipolarization in Saturn's magnetotail with planetward ion flows and energetic particle flow bursts: Evidence of quasi-steady reconnection. *Journal of Geophysical Research*, *120*(5), 3603–3617. https://doi.org/10.1002/2015JA020995

Kanani, S. J., Arridge, C. S., Jones, G. H., Fazakerley, A. N., McAndrews, H. J., Sergis, N., et al. (2010). A new form of Saturn's magnetopause using a dynamic pressure balance model, based on in situ, multi-instrument cassini measurements. *Journal of Geophysical Research*, *115*, A06207. https://doi.org/10.1029/2009JA014262

Keiling, A., Thaller, S., Wygant, J., & Dombeck, J. (2019). Assessing the global alfven wave power flow into and out of the auroral acceleration region during geomagnetic storms. *Science Advances*, *5*(6), eaav8411. https://doi.org/10.1126/sciadv.aav8411

Keiling, A., Wygant, J., Cattell, C., Mozer, F., & Russell, C. (2003). The global morphology of wave Poynting flux: Powering the aurora. *Science*, *299*(5605), 383–386. https://doi.org/10.1126/science.1080073

Kleindienst, G., Glassmeier, K. H., Simon, S., Dougherty, M. K., & Krupp, N. (2009). Quasiperiodic ulf-pulsations in saturn's magnetosphere. *Annales Geophysicae*, *27*(2), 885–894. https://doi.org/10.5194/angeo-27-885-2009

Lee, D., & Lysak, R. (1989). Magnetospheric ulf wave coupling in the dipole model—The impulsive excitation. *Journal of Geophysical Research*, *94*(A12), 17097. https://doi.org/10.1029/JA094iA12p17097

Lepping, R., Burlaga, L., & Klein, L. (1981). Surface-waves on Saturns magnetopause. *Nature*, *292*(5825), 750–753. https://doi.org/10.1038/292750a0

Lomb, N. (1976). Least-squares frequency-analysis of unequally spaced data. *Astrophysics and Space Science*, *39*(2), 447–462. https://doi.org/10.1007/BF00648343

Masters, A., Achilleos, N., Bertucci, C., Dougherty, M. K., Kanani, S. J., Arridge, C. S., et al. (2009). Surface waves on Saturn's dawn flank magnetopause driven by the kelvin-helmholtz instability. *Planetary and Space Science*, *57*(14–15), 1769–1778. https://doi.org/10.1016/j.pss.2009.02.010

Masters, A., Achilleos, N., Cutler, J., Coates, A., Dougherty, M., & Jones, G. (2012). Surface waves on Saturn's magnetopause. *Planetary and Space Science*, *65*(1), 109–121. https://doi.org/10.1016/j.pss.2012.02.007

Masters, A., Achilleos, N., Kivelson, M. G., Sergis, N., Dougherty, M. K., Thomsen, M. F., et al. (2010). Cassini observations of a Kelvin-Helmholtz vortex in Saturn's outer magnetosphere. *Journal of Geophysical Research*, *115*, A07225. https://doi.org/10.1029/2010JA015351

Palmaerts, B., Radioti, A., Roussos, E., Grodent, D., Gerard, J. C., Krupp, N., & Mitchell, D. G. (2016). Pulsations of the polar cusp aurora at Saturn. *Journal of Geophysical Research*, *121*(12), 11952–11963. https://doi.org/10.1002/2016JA023497

Palmaerts, B., Roussos, E., Krupp, N., Kurth, W. S., Mitchell, D. G., & Yates, J. N. (2016). Statistical analysis and multi-instrument overview of the quasi-periodic 1-hour pulsations in Saturn's outer magnetosphere. *Icarus*, *271*, 1–18. https://doi.org/10.1016/j.icarus.2016.01.025

Radioti, A., Grodent, D., Yao, Z. H., Gerard, J. C., Badman, S. V., Pryor, W., & Bonfond, B. (2017). Dawn auroral breakup at Saturn initiated by auroral arcs: Uvis/cassini beginning of grand finale phase. *Journal of Geophysical Research*, *122*(12), 12111–12119. https://doi.org/10.1002/2017JA024653

Radioti, A., Yao, Z., Grodent, D., Palmaerts, B., Roussos, E., Dialynas, K., Bonfond, et al. (2019). Auroral beads at Saturn and the driving mechanism: Cassini proximal orbits. *The Astrophysical Journal Letters*, *885*(1), L16. https://doi.org/10.3847/2041-8213/ab4e20

Roussos, E., Krupp, N., Mitchell, D. G., Paranicas, C., Krimigis, S. M., Andriopoulou, M., et al. (2016). Quasi-periodic injections of relativistic electrons in Saturn's outer magnetosphere. *Icarus*, *263*(SI), 101–116. https://doi.org/10.1016/j.icarus.2015.04.017

Russell, C., Khurana, K., Huddleston, D., & Kivelson, M. (1998). Localized reconnection in the near jovian magnetotail. *Science*, *280*(5366), 1061–1064. https://doi.org/10.1126/science.280.5366.1061

Saur, J., Janser, S., Schreiner, A., Clark, G., Mauk, B. H., Kollmann, P., et al. (2018). Wave-particle interaction of Alfven waves in Jupiter's magnetosphere: Auroral and magnetospheric particle acceleration. *Journal of Geophysical Research: Space Physics*, *123*(11), 9560–9573. https://doi.org/10.1029/2018JA025948

Scargle, J. (1982). Studies in astronomical time-series analysis 2. statistical aspects of spectral-analysis of unevenly spaced data. *The Astrophysical Journal*, *263*(2), 835–853. https://doi.org/10.1086/160554

Slavin, J. A., Acuna, M. H., Anderson, B. J., Baker, D. N., Benna, M., Boardsen, S. A., et al. (2009). Messenger observations of magnetic reconnection in Mercury's magnetosphere. *Science*, *324*(5927), 606–610. https://doi.org/10.1126/science.1172011

Sun, W.-J., Slavin, J. A., Fu, S., Raines, J. M., Zong, Q.-G., Imber, S. M., et al. (2015). Messenger observations of magnetospheric substorm activity in mercury's near magnetotail. *Geophysical Research Letters*, *42*(10), 3692–3699. https://doi.org/10.1002/2015GL064052

Vogt, M. F., Kivelson, M. G., Khurana, K. K., Joy, S. P., & Walker, R. J. (2010). Reconnection and flows in the jovian magnetotail as inferred from magnetometer observations. *Journal of Geophysical Research*, *115*, A06219. https://doi.org/10.1029/2009JA015098

Waite, J., Combi, M., Ip, W., Cravens, T., McNutt, R., Kasprzak, W., et al. (2006). Cassini ion and neutral mass spectrometer: Enceladus plume composition and structure. *Science*, *311*(5766), 1419–1422. https://doi.org/10.1126/science.1121290

Wilson, R. J., Delamere, P. A., Bagenal, F., & Masters, A. (2012). Kelvin-helmholtz instability at Saturn's magnetopause: Cassini ion data analysis. *Journal of Geophysical Research*, *117*(A3), A03212. https://doi.org/10.1029/2011JA016723

Yao, Z. H., Grodent, D., Kurth, W. S., Clark, G., Mauk, B. H., Kimura, T., et al. (2019). On the relation between Jovian aurorae and the loading/unloading of the magnetic flux: Simultaneous measurements from Juno, hubble space telescope, and hisaki. *Geophysical Research Letters*, *46*(21), 11632–11641. https://doi.org/10.1029/2019GL084201

Yao, Z. H., Grodent, D., Ray, L. C., Rae, I. J., Coates, A. J., Pu, Z. Y., et al. (2017). Two fundamentally different drivers of dipolarizations at Saturn. *Journal of Geophysical Research: Space Physics*, *122*(4), 4348–4356. https://doi.org/10.1002/2017JA024060

Yao, Z., Pu, Z. Y., Rae, I. J., Radioti, A., & Kubyshkina, M. V. (2017). Auroral streamer and its role in driving wave-like pre-onset aurora. *Geoscience Letters*, *4*(1), 8. https://doi.org/10.1186/s40562-017-0075-6

Yao, Z. H., Radioti, A., Rae, I. J., Liu, J., Grodent, D., Ray, L. C., et al. (2017). Mechanisms of Saturn's near-noon transient aurora: In situ evidence from Cassini measurements. *Geophysical Research Letters*, *44*(22), 11217–11228. https://doi.org/10.1002/2017GL075108

Young, D. T., Berthelier, J. J., Blanc, M., Burch, J. L., Coates, A. J., Goldstein, R., et al. (2004). Cassini plasma spectrometer investigation. *Space Science Reviews*, *114*(1–4), 1–112. https://doi.org/10.1007/s11214-004-1406-4

Zhao, H., Zhou, X.-Z., Liu, Y., Zong, Q.-G., Rankin, R., Wang, Y., et al. (2019). Poleward-moving recurrent auroral arcs associated with impulse-excited standing hydromagnetic waves. *Earth and Planetary Physics*, *3*(4), 305–313. https://doi.org/10.26464/epp2019032

Zong, Q., Rankin, R., & Zhou, X. (2017). The interaction of ultra-low-frequency pc3-5 waves with charged particles in Earth's magnetosphere. *Reviews of Modern Plasma Physics*, *1*(1), 10. https://doi.org/10.1007/s41614-017-0011-4

Zong, Q.-G., Zhou, X.-Z., Wang, Y. F., Li, X., Song, P., Baker, D. N., et al. (2009). Energetic electron response to ulf waves induced by interplanetary shocks in the outer radiation belt. *Journal of Geophysical Research*, *114*, A10204. https://doi.org/10.1029/2009JA014393